Hydroxyl and sulfate radicals activated by Fe(III)-EDDS/UV: Comparison of their degradation efficiencies and influence of critical parameters

Xiaoning Wang, Wenbo Dong, Marcello Brigante, Gilles Mailhot

INVITATION LETTER

Dear Colleague,

You are invited to participate to the Special Issue (SI) on "Light-Assisted Catalysis for Water and Wastewater Treatment" (LACWWT) to be published in Applied Catalysis B: Environmental (IF 2016 =9.44) honoring the retirement of Professor César Pulgarin.

Remember that article title and authors MUST be that provided by you to the invited editors, or very similar. No other paper will be admitted.

The deadline for manuscript submission is **September 30, 2018 (NO EXTENSION WILL BE ALLOWED)**.

All the manuscripts should follow the guidelines of *Applied Catalysis B: Environmental,* will undergo the regular peer-review process and should meet the highest scientific quality standards of the journal. Manuscripts should be submitted online through EES system (https://ees.elsevier.com/apcatb/). You must choose Article Type as "Special issue - Honoring Cesar Pulgarin (LACWWT)" during the submission process. **Please include this "Invitation Letter" from the Guest Editors along with the manuscript**. For more general information please visit the online "Instructions for Authors" on: https://www.elsevier.com/journals/applied-catalysis-b-environmental/0926-3373/guide-for-authors.

SPECIFIC INSTRUCTIONS. The maximum length of each article is 8000 words equivalent (including abstract, text, figures, tables and references). A figure or table is equivalent to 400 words. Include in your COVER LETTER the contact e-mail of all co-authors and FOUR possible referees for your paper. Remember that perhaps you will be contacted by editors to actuate as referee of other papers of the SI.

This sentence should be added in the **Acknowledgements** section of their contributions stating: *"This Special Issue is dedicated to honor the retirement of Prof. César Pulgarin at the Swiss Federal Institute of Technology (EPFL, Switzerland), a key figure in the area of Catalytic Advanced Oxidation Processes".* As this SI is devoted to the closing of the career of Prof. Pulgarin, authors are also highly welcome to mention how their research and vision of AOPs has been affected by the works of Prof. Cesar Pulgarin.

Yours sincerely,

Prof. Sixto Malato Rodriguez
CIEMAT-Plataforma Solar de Almería, Spain. sixto.malato@psa.es

Prof. Ricardo Antonio Torres-Palma
Instituto de Química - Universidad de Antioquia, Colombia. ricardo.torres@udea.edu.co

Dr. Stefanos Giannakis
Swiss Federal Institute of Technology (EPFL), Switzerland. stefanos.giannakis@epfl.ch

Dr. Sami Rtimi
Swiss Federal Institute of Technology (EPFL), Switzerland. sami.rtimi@epfl.ch

Hydroxyl and sulfate radicals activated by Fe(III)-EDDS/UV : comparison of their degradation efficiencies and influence of critical parameters

Xiaoning Wang [a, b, c], Wenbo Dong [b], Marcello Brigante [a], Gilles Mailhot [a*]

[a] Université Clermont Auvergne, CNRS, SIGMA Clermont, Institut de Chimie de Clermont-Ferrand, F-63000 Clermont-Ferrand, France

[b] Shanghai Key Laboratory of Atmospheric Particle Pollution and Prevention, Department of Environmental Science and Engineering, Fudan University, Shanghai 200433, China

[c] Suzhou Key Laboratory of Green Chemical Engineering, School of Chemical and Environmental Engineering, College of Chemistry, Chemical Engineering and Materials Science, Soochow University, Suzhou, Jiangsu 215123, China

* Corresponding author: gilles. mailhot@uca.fr

Abstract

In the present study, comparison of activation efficiencies of hydrogen peroxide (H_2O_2) and persulfate (PS, $Na_2S_2O_8$) induced by Fe(III)-Ethylenediamine-*N*,*N'*-disuccinic acid (EDDS) under polychromatic irradiation UVA and visible region at same conditions was studied for the first time. The effects of pH, Fe(III)-EDDS concentration, H_2O_2 and PS concentrations were investigated. *p*-hydroxyphenylacetic acid (*p*-HPA) was taken as a model pharmaceutical intermediate pollutant to estimate the oxidative process efficiency. In these two systems, the degradation rate of *p*-HPA increased (not linearly) using higher concentrated solution of H_2O_2 and $Na_2S_2O_8$. However, when

Fe(III)-EDDS concentration exceeding 250 μM, the degradation efficiency of *p*-HPA began to decrease. Surprisingly, results of pH effects showed that Fe(III)-EDDS/H_2O_2/UV system presents much higher degradation efficiency than Fe(III)-EDDS/PS/UV whatever the solution pH's, especially in neutral and alkaline solutions. In the Fe(III)-EDDS/H_2O_2/UV reaction, *p*-HPA degradation rate ($R_{p\text{-HPA}}$) increased fast from pH 2.5 to 7.5, then it began to decrease when pH increased to 9.0. While $R_{p\text{-HPA}}$ started to decrease with pH increase to 3.9 in Fe(III)-EDDS/PS/UV system. To explain this phenomenon, the second order constant of *p*-HPA (for both molecular and mono-anionic forms) with $HO^{\bullet}$ and $SO_4^{\bullet-}$ radicals were determined by laser flash photolysis (LFP) experiments for the first time. Results showed that $k_{p-HPA,HO^{\bullet}}$ was higher than $k_{p-HPA,SO_4^{\bullet-}}$ for both anionic and molecular forms of pollutant. These results demonstrated that iron-complex induced photo-Fenton process is more efficient than activation of persulfate process, particularly at environmentally closed pH values and sun-simulated wavelengths (λ > 300 nm).

Keywords

Advanced oxidation processes, iron-EDDS complexes, decontamination, wastewater

1. Introduction

Wastewater treatments based on advanced oxidation processes (AOPs), which mainly depend on the generation of free radical species, have been extensively studied in the last two decades [1, 2]. The reaction between H_2O_2 and Fe(II)/Fe(III) is a well-known method for the generation of hydroxyl radicals ($HO^{\bullet}$), including Fenton (Fe(II)/H_2O_2) [3, 4], Fenton-like (Fe(III)/H_2O_2) [5] and photo-Fenton (UV/Fe(III)/H_2O_2) processes [6-10]. With high oxidation abilities, $HO^{\bullet}$ (E^0 = 2.8 V)

has a wide application for removing environmental contaminants like endocrine disruptors, chlorophenols, dyes, pharmaceuticals and pesticides [4, 11-13]. However, in recent years, studies on sulfate radical ($SO_4^{\bullet-}$) have proved that this radical is outstanding in degrading recalcitrant organic pollutants ascribing to its similar oxidation-reduction potential (E^0 = 2.6-3.2 V) [14], much longer half-life time and more selective reactivity compared with $HO^{\bullet}$. From previously reported literature data, the generation of $SO_4^{\bullet-}$ usually derives from the activation of persulfate (PS) by heat [15], UV or transition metals [16-18]. Among these activation processes, methods involved Fe^0, Fe^{2+} or Fe^{3+} with or without UV are efficient, energy-saving and relatively nontoxic [18]. The main formations of $HO^{\bullet}$ and $SO_4^{\bullet-}$, from iron activation routes, are shown below [19-21]:

$Fe^{2+}+H_2O_2 \rightarrow Fe^{3+}+HO^{\bullet}+OH^-$ $\quad k_1 = 76\ M^{-1}\ s^{-1}$ (R1)

$Fe^{3+}+H_2O_2 \rightarrow Fe^{2+}+HO_2^{\bullet}+H^+$ $\quad k_2 = 0.02\ M^{-1}\ s^{-1}$ (R2)

$S_2O_8^{2-}+Fe^{2+} \rightarrow SO_4^{\bullet-}+SO_4^{2-}+Fe^{3+}$ $\quad k_3 = 20\text{-}27\ M^{-1}\ s^{-1}$ (R3)

The generation of $HO^{\bullet}$ and $SO_4^{\bullet-}$ based on iron mediated activation, mainly combined with UV irradiation, has played predominant roles in advanced oxidation processes. However, there are several defects in these activation methods. The most predominant drawback is the Fe^{2+} natural oxidation into Fe^{3+} in water due to the oxygen presence and Fe^{3+} ions precipitation at pH higher than 4.0. Therefore, most of the iron species present in natural and slightly basic solutions, exist in the form of insoluble ferric oxides and (hydr)oxides. Due to these physicochemical properties of iron in water, the activation of persulfate by Fe^{2+}/Fe^0 is more favorable in acidic solution than in neutral and alkaline pH [18].

For these reasons, the development of Fe(III)/Fe(II) organic complexes is essential to improve the removal efficiencies under environmentally relevant pH values. Polycarboxylate acids like citric,

oxalic and aminopolycarboxylic acids like ethylenediaminetetraacetic acid (EDTA) can form stable water soluble complexes with iron in neutral and slightly basic pH solutions, enhancing the dissolution of iron in natural water. Moreover, these complexes are photochemicaly active and efficient leading, by photoredox process, to the production of oxidative species like hydroxyl radicals [13, 22, 23]. However, EDTA is toxic and hard to be removed from aqueous solution by traditional chemical and biological water treatments and so it is always found in considerable concentration in rivers [24]. Compared to EDTA, ethylenediamine-N,N′-disuccinic acid (EDDS), which is a structural isomer of EDTA, has been recognized to be more easily biodegraded and more environmental friendly [25]. Photo-induced production of $HO^{\bullet}$ and $SO_4^{\bullet-}$ based on Fe(II)/Fe(III)-EDDS complexes has been widely studied in recent years, showing excellent efficiency in removing organic pollutants in water and soil near neutral pH [5, 7, 9, 26-33]. Huang et al. demonstrated that in homogeneous Fenton-like process (Fe(III)-EDDS/H_2O_2), Fe(III)-EDDS (molar ration 1:1) shows better removal efficiency of bispenol A (BPA) in alkaline solution than in acidic one [34]. At the same time, Wu and coworkers reported that under UV radiation, photo-Fenton process (Fe(III)-EDDS/H_2O_2/UV) has much higher efficiency in removing 4-tert-Butylphenol (4tBP) than Fenton process. This result can be ascribed to the rapid generation of Fe(II) under irradiation [9]. In the presence of PS with Fe(III)-EDDS/UV, rapid oxidation of 4-terbutylphenol (4tBP) is observed due to the formation of $SO_4^{\bullet-}$. In neutral and basic pH conditions, the efficiency of 4tBP degradation is much higher with Fe(III)-EDDS than with Fe(III) aquacomplexes [14]. So, the use of Fe(III)-EDDS complexes leads to efficient oxidation processes whatever the sources of radical species ($HO^{\bullet}$ or $SO_4^{\bullet-}$). However, the comparison between Fe(III)-EDDS/H_2O_2/UV and Fe(III)-EDDS/PS/UV systems under same conditions including the

effects of pH, Fe(III)-EDDS concentration, H_2O_2 and PS concentrations has never been investigated before. The main goal of this paper is to compare these two processes using *p*-hydroxyphenylacetic acid (*p*-HPA) as a model pollutant. *p*-HPA is one of the pharmaceutical intermediates and also widely used in the synthesis of pesticides and commonly detected in olive oil wastewaters [35, 36]. The aim of this study is to quantify the different activation efficiency of H_2O_2 and PS by Fe(III)-EDDS under irradiation in the same experimental conditions and to correlate the efficiency with the production of $HO^{\bullet}$ and $SO_4^{\bullet-}$ radicals. Especially, to reach this goal and understand the different mechanisms, the second order rate constants of *p*-HPA with $HO^{\bullet}$ and $SO_4^{\bullet-}$ are determined by laser flash photolysis (LFP) for the first time.

2. Materials and methods

2.1 Irradiation setup and experimental procedure

List of chemicals used in this work is reported in the Supporting Information. For the control experiment in the dark, reactions are performed in a brown bottle with continuous magnetic stirring at room temperature. The reactions start from the addition of H_2O_2 or $Na_2S_2O_8$ to the solution. For the degradation of *p*-HPA under irradiation, the experiments are performed in a home-made photoreactor placed in a cylindrical stainless steel container. Four fluorescent light bulb lamps (Philips TL D 15 W/05) were separately placed in four different axes. Meanwhile, the photoreactor, which is a water-jacketed Pyrex tube with 2.8 cm internal diameter, was placed at the center of the setup. The emission spectrum (Fig.S1) was determined using an optical fiber coupled with a CCD spectrophotometer (Ocean Optics USD 2000+UV−vis) and energy has been normalized to the actinometry results using paranitroanisole (PNA)/pyridine method [37]. A total

flux of 1451 W m^{-2} reaching the solution was determined between 300–500 nm. Solutions are magnetically stirred with a magnetic bar during the reaction and total volume was 100 mL. All the experiments are carried out at room temperature (293±2 K), controlled by a circulating cooling water system. The initial concentration of *p*-HPA is 50 µM in all experiments, and samples are taken from the reaction tube at fixed interval times. In order to stop the Fenton reaction after the samples taken from the photoreactor, 20 µL IPA were added immediately after withdrawn.

2.2 p-HPA quantification and degradation rate

The concentration of the *p*-HPA remaining in the aqueous solution is determined with an Alliance high performance liquid chromatography (HPLC) equipped with a photodiode array detector (Waters 2998, USA) and Waters 2695 separations module. The experiments are performed by UV detection at 274 nm. The flow rate is 0.15 mL min^{-1}, the injection volume is 50 µL and the mobile phase is a mixture of water (with 0.1% H_3PO_4) and methanol (65/35, v/v). The column is a Nucleodur 100-3 C18 of 150 × 2.0 mm, particle size 3 µm. In these conditions, the retention time of *p*-HPA is 6.7 min.The initial degradation rate of *p*-HPA is $R_{p\text{-HPA}}$ (M s^{-1}) = k_{app}× $[p\text{-HPA}]_0$ with $[p\text{-HPA}]_0$ the initial concentration of *p*-HPA, k_{app} the pseudo-first-order apparent rate constant (s^{-1}). The error is ±3σ, obtained from the scattering of the experimental data.

2.3 Laser Flash Photolysis

Experiments are carried out using the fourth harmonic (λ_{exc} = 266 nm) of a Quanta Ray GCR 130-01 Nd: YAG laser system instrument and the energy is set at 45 mJ/pulse. Other conditions are kept the same to those described in previous articles [14, 38]. Conditions and chemicals used for the determination of reactivity constants are reported in the Supplementary Information.

3. Results and Discussion

3.1 Evaluation of the second order rate constants

p-HPA has two pKa (4.5 and 10.5) corresponding to the carbonyl and alcoholic functions. Considering that the typical pH range of natural and sewage treatment plan waters is from 4 to 8, the second second-order rate constant was determined at pH 2.5 (molecular form) and pH 8.5 (mono-anionic form). At 266 nm laser excitation no transient species are detected when only *p*-HPA is present in solution. The determination of the second order rate constant between *p*-HPA and $HO^{\bullet}$ ($k_{p-HPA,HO^{\bullet}}$) is determined by using chemical competition kinetics with thiocyanate anions (SCN^{-}) as reported in equations R4-R7 and Scheme S1. $k_{p-HPA,HO^{\bullet}}$ is obtained by following the absorbance of $SCN_2^{\bullet-}$ in the presence of different *p*-HPA concentrations. The absorbance of $SCN_2^{\bullet-}$ species decreases when the concentration of *p*-HPA increases due to the competition with SCN^{-} for the reaction of $HO^{\bullet}$. The slope of the linear fit of Abs_0/Abs *vs p*-HPA concentration is used to determine the second order rate constant $k_{p-HPA,HO^{\bullet}}$ (Table 1). Details concerning the second-order rate constant determination are reported in Fig. S2A.

$$H_2O_2 \xrightarrow{h\nu} 2HO^{\bullet} \qquad \text{(R4)}$$

$$HO^{\bullet} + p-HPA \xrightarrow{k_{p-HPA,HO^{\bullet}}} products \qquad \text{(R5)}$$

$$HO^{\bullet} + SCN^{-} \rightarrow HO^{-} + SCN^{\bullet} \qquad \text{(R6)}$$

$$SCN^{\bullet} + SCN^{-} \rightarrow SCN_2^{\bullet-} \qquad \text{(R7)}$$

For sulfate radical reactivity, the decay of $SO_4^{\bullet-}$ was followed at 450 nm. To obtain $k_{p-HPA,SO_4^{\bullet-}}$, the pseudo-first order constant decay of $SO_4^{\bullet-}$ ($k'_{SO_4^{\bullet-}}$) in the presence of different *p*-HPA concentrations was fit with a linear equation. The slope was the $k_{p-HPA,SO_4^{\bullet-}}$ value [14]. At pH 2.5, a decrease of the $SO_4^{\bullet-}$ was observed with a pseudo-first order constant $k'_{SO_4^{\bullet-}}$ of 4.29×10^4 s^{-1}.

After the addition of *p*-HPA (3.33×10^{-4} M), the transient decay increases to 1.58×10^{6} s^{-1} due to the quenching of $SO_4^{\bullet-}$ by *p*-HPA (Fig. S2B). The same method was used at pH 8.5 for the reactivity of mono-anionic form of *p* -HPA and the results are reported in Table 1. In acidic solution (molecular form of *p*-HPA) the reactivity between *p*-HPA and photogenerated radicals results higher than at alkaline pH (mono-anionic form of *p*-HPA). This effect is more pronounced with $HO^{\bullet}$ where $k_{p-HPA,HO^{\bullet}}$ is 3 times higher at pH 2.5 than at pH 8.5, while for $SO_4^{\bullet-}$ an increase of about 1.3 times is determined.

3.2 Effect of UV and Fe(III)-EDDS complex

In the dark, *p*-HPA is stable in aqueous solution even in the presence of Fe(III)-EDDS and no direct photolysis was observed under adopted irradiation conditions. As a contrary, under adopted UVA polychromatic irradiation, H_2O_2 and $Na_2S_2O_8$ can produce $HO^{\bullet}$ (R4) and $SO_4^{\bullet-}$ (R8).

$$S_2O_8^{2-} \xrightarrow{h\nu} 2SO_4^{\bullet-} \qquad \text{(R8)}$$

$$Fe(III)-EDDS + H_2O_2 \rightarrow Fe(II)-EDDS + HO_2^{\bullet} / O_2^{\bullet-} + H^+ \qquad \text{(R9)}$$

$$Fe(III)-EDDS \xrightarrow{h\nu} Fe(II) + EDDS^{\bullet} \qquad \text{(R10)}$$

However, *p*-HPA has a relatively low degradation rate in the presence of H_2O_2 (1 mM) or $Na_2S_2O_8$ (1 mM) alone under UV, achieving 10% and 30% removal respectively, after 120 min of irradiation (Fig. S3 and S4). In fact, the quantum yield of HO• generation is very low at wavelengths longer than 300 nm. In terms of pH effect, faster *p*-HPA degradation is observed at pH 3.0 or 4.5 than at pH 9.4 in agreement with the evaluated second order rate constants as a function of pH (Table 1).

Fig.1A shows the degradation of *p*-HPA with Fe(III)-EDDS (100 μM) at two different H_2O_2

concentrations (100 and 500 µM) in the dark or under irradiation. The disappearance of *p*-HPA is much faster in the photo-Fenton system (Fe(III)-EDDS/H_2O_2/UV) than in Fenton-like process (Fe(III)-EDDS/H_2O_2) [34]. According to the summarized mechanism (see before), the production of $HO^{\bullet}$ was correlated with the formation of Fe(II) (R9, R10) [9, 34] and then with the oxidation of target compound. Under irradiation, UVA light significantly enhances the generation of Fe(II), improving the degradation of *p*-HPA in the first 10 min through the Fenton process (R1) [7, 9]. At higher H_2O_2 concentration (500 µM) added into the solution, *p*-HPA can be removed completely in 60 min in Fenton-like process and in 10 min in photo-Fenton system. At lower concentration of H_2O_2 (100 µM) *p*-HPA is not completely removed with or without UV irradiation. These results corroborate that H_2O_2 concentration is a crucial and a limiting parameter in the oxidation process.

With $Na_2S_2O_8$, the pH and the different concentrations are kept the same of the H_2O_2 system. The different degradation kinetics are shown in Fig.1B. Although some previous papers reported that Fe(III) can activate persulfate to produce $SO_4^{\bullet -}$ in the dark, it was not the case in our system. In fact, much higher concentration of Fe(III) species and persulfate seem needed to do this activation [39]. Under irradiation, Fe(III)-EDDS/$Na_2S_2O_8$ system shows a good efficiency for *p*-HPA degradation but much lower compared to the system with H_2O_2. Different reasons can explain the lower efficiency of this system. First of all, it is important to mention that the formation of Fe(II) *via* reaction R10 is one of the crucial step to active $S_2O_8^{2-}$ or H_2O_2 to produce oxidative species through reactions R1 and R3, which are identified and evaluated in terms of relative importance in the following part of this paper. The lower efficiency can be due to the fact that the second order rate constant of the activation of $S_2O_8^{2-}$ ($k_{S_2O_8^{2-},Fe^{2+}}$ = 20-27 M^{-1} s^{-1}) is more than three times smaller than the one with H_2O_2 ($k_{H_2O_2,Fe^{2+}}$ = 76 M^{-1} s^{-1}). In addition, the lower efficiency of

$Na_2S_2O_8$ can be also due to the second order rate constants between *p*-HPA with $HO^{\bullet}$ or $SO_4^{\bullet-}$, $k_{p-HPA,HO^{\bullet}}$ is 4.6 times higher than $k_{p-HPA,SO_4^{\bullet-}}$ in acidic solutions (Table 1). As a contrary, the photolysis of H_2O_2 and $Na_2S_2O_8$ are not responsible for this effect at the concentration and light irradiation wavelengths used in this process.

3.3 Effects of H_2O_2 and $Na_2S_2O_8$ concentrations

Initial degradation rate of *p*-HPA ($R_{p\text{-HPA}}$) is used to evaluate the degradation efficiency of the reaction process. $R_{p\text{-HPA}}$ is evaluated from the first 5 min of irradiation, because during this period pH of the solution kept stable, and the degradation can be well fitted by pseudo first order kinetics. Fig.2 shows the initial degradation rate of *p*-HPA with different H_2O_2 concentrations in photo-Fenton process. $R_{p\text{-HPA}}$ increases from 1.50×10^{-7} to 3.80×10^{-7} M s^{-1} when H_2O_2 concentrations increases from 50 μM to 1 mM. The observed increase of *p*-HPA degradation when the concentration of H_2O_2 increased is obvious considering that H_2O_2 is one of the two compounds generating $HO^{\bullet}$ in the Fenton process. In fact, as described in Fig.1A, H_2O_2 concentration was the limiting parameter. However, H_2O_2 is also a scavenger of $HO^{\bullet}$ ($k_{H_2O_2,HO^{\bullet}}$ = 2.7×10^{7} M^{-1} s^{-1}) and so too high concentration of H_2O_2 will lead to a decrease of the organic compound degradation rate [7]. Due to the much higher rate constant of $HO^{\bullet}$ reaction on *p*-HPA ($k_{p-HPA,HO^{\bullet}}$ = 2.2×10^{10} $M^{-1}s^{-1}$) the decrease of the *p*-HPA degradation is not observed in our experimental conditions. In fact at highest H_2O_2 concentration used (1 mM) 90% of $HO^{\bullet}$ are still consumed by *p*-HPA. For this reason, it was only observed that the increase rate slowed down when H_2O_2 increased from 250 μM to 1 mM. Moreover, at this concentration the contribution to the degradation of *p*-HPA from the direct photolysis of H_2O_2 is still negligible (Fig. S3).

The effect of $Na_2S_2O_8$ concentration is shown in Fig.2. Similar to H_2O_2, the degradation rate is always increasing when $Na_2S_2O_8$ concentration increases. In fact $S_2O_8^{2-}$ is the source of radical species and the negative effect of $Na_2S_2O_8$, in terms of radical species scavenger probably $SO_4^{\bullet-}$ in this case ($k_{S_2O_8^{2-},SO_4^{\bullet-}}$ = 6.1×10^5 M^{-1} s^{-1}) [40], is much slower than in the case with H_2O_2 ($k_{H_2O_2,HO^\bullet}$ = 2.7×10^7 M^{-1} s^{-1}). In fact, under our experimental conditions ([$Na_2S_2O_8^{2-}$] ≤ 1 mM) a constant increase of the degradation rate of *p*-HPA with the increase of persulfate concentration is observed.

3.4 Effects of Fe(III)-EDDS concentrations

Fig.3 shows the removal percentage of *p*-HPA with different Fe(III)-EDDS concentrations after 5 min of irradiation in the presence of 100 μM of H_2O_2. The removal percentage of *p*-HPA increases when Fe(III)-EDDS concentration increases from 50 to 250 μM and a decreases at higher Fe(III)-EDDS concentration up to 1 mM is observed. Higher concentration of Fe(III)-EDDS produces larger amount of Fe(II) under irradiation followed with higher concentration of $HO^\bullet$ through Fenton process. However, EDDS is able to interact with this process. Compared with H_2O_2, EDDS has an almost 100 times higher second order rate constant with $HO^\bullet$ ($k_{EDDS,HO^\bullet}$ = $2.48\pm0.43\times10^9$ M^{-1} s^{-1} >> $k_{H_2O_2,HO^\bullet}$) [41]. Moreover, by similarity of the results published by Di Somma et al. [42] on Cu(II)-EDDS complex, Fe(III)-EDDS could be also a significant trap of hydroxyl radicals. So, EDDS, its photo-induced by-products and Fe(III)-EDDS complex can compete more strongly with *p*-HPA molecules. Another reason can explain the inhibition at higher Fe(III)-EDDS concentration. In fact, Fe(III)-EDDS is decomposed very fast under irradiation [17, 30], and the high concentration of Fe(II) produced is able to react with $HO^\bullet$

with a high reaction rate (R11) [43]. Furthermore, the formed Fe(III) species are spontaneously precipitated at the used pH (7.5). Thus the formed colloid or precipitation can be responsible for the inhibition of the penetration of photons in the solution.

In Fe(III)-EDDS/$Na_2S_2O_8$/UV system, $Na_2S_2O_8$ is set as 500 μM, because at lower concentration (100 μM), it is difficult to differentiate the effect of Fe(III)-EDDS concentration due to relatively low degradation percentages. From Fig.3, a similar trend can be observed compared to H_2O_2, so EDDS and its by-product also act as scavengers of $SO_4^{\bullet-}$ ($k_{EDDS,SO_4^{\bullet-}} = 6.21\times10^9$ $M^{-1}s^{-1}$) [14]. Moreover, higher concentration of Fe(III)-EDDS can produce high concentration of Fe(II) in solution at the initial stage, while too much Fe(II) also can compete reacting with $SO_4^{\bullet-}$ with high rate constant (R12) [16].

$Fe(II) + HO^{\bullet} \rightarrow Fe(III) + OH^-$ $\quad k_{Fe2+,HO\bullet} = 3.2\times10^8\ M^{-1}s^{-1}$ (R11)

$Fe(II) + SO_4^{\bullet-} \rightarrow Fe(III) + SO_4^{2-}$ $\quad k_{Fe^{2+},SO_4^{\bullet-}} = 4.6\times10^9\ M^{-1}s^{-1}$ (R12)

3.5 Effects of pH

In the Fe(III) (photo)-induced activation reactions, pH always plays a significant role during the whole process. Firstly, in the *p*-HPA/Fe(III)-EDDS/UV system, pH effects are investigated, as shown in the insert of Fig.4. Under polychromatic irradiation, Fe(III)-EDDS can produce HO• through a complex photoinduced mechanism as described in different studies [17, 44]. However, if we compare with the photo-Fenton process, the photo-production of HO• was very limited without H_2O_2. (Fig.1). When the pH increases from 3.0 to 4.7, the removal efficiency increases very fast, while with pH further increase up to 9.4, degradation percentage continues to increase but much more slowly. The constant increase of the *p*-HPA removal with the increase of pH is due

to the higher $HO^{\bullet}$ formation quantum yield when the pH increases [17]. However, according to our previous results by Wu et al. [14, 30], Fe(III)-EDDS showed different predominant species with respect to pH and the complex Fe(OH)EDDS formed at pH higher than 6.0 can also explain the higher efficiency at higher pH in terms of $HO^{\bullet}$ formation. However, the slower increase observed at pH higher than 4.7, can be attributed to the lower reactivity (three times lower) of $HO^{\bullet}$ on the mono-anionic form of *p*-HPA. The rate constants have been evaluated for the first time during this study and are presented in Table 1.

The pH effect on the Fe(III)-EDDS/H_2O_2/UV and Fe(III)-EDDS/$Na_2S_2O_8$/UV processes during the initial stage (first 5 min of irradiation) are shown in Fig.4. The trend of pH effects is different from Fe(III)-EDDS/UV system and is also quite different although the experimental conditions are similar but the oxidation species used (H_2O_2 and $Na_2S_2O_8$) are different. So, the activation mechanisms of these two different processes are not exactly the same.

In the Fe(III)-EDDS/H_2O_2/UV reaction, *p*-HPA degradation efficiency increases fast from pH 2.5 to 7.5, then it begins to decrease when pH increases to 9.0. As explained with the system Fe(III)-EDDS/UV (insert Fig.4), in general, the increase of efficiency with the increase of pH is mainly due to the increased $HO^{\bullet}$ formation quantum yield and chemical speciation of Fe(III)-EDDS complexes vs pH possessing different photoactive abilities. However, in the photo-Fenton process $HO^{\bullet}$ generation is mainly due to the Fenton process and so to the photo-generation of Fe(II) which is correlated with the first photochemical step, the photoredox process from the complex Fe(III)-EDDS leading to the formation $EDDS^{\bullet}$ and Fe(II). To compare and understand well this mechanism, Fe^{3+} is introduced instead of Fe(III)-EDDS, see Fig.S5. In order to keep Fe^{3+} soluble in the solution, a very acidic pH is selected (pH = 2.0) although the

optimal pH is 2.8 to better generate the most light absorbing iron complex with water molecules. Fe(III)-EDDS shows faster degradation efficiency than Fe^{3+} in the initial stage, ascribing to the higher photochemical activity of the complex Fe(III)-EDDS than the ion Fe^{3+}. As for Fe(III)-EDDS, the degradation is also very fast in the first 10 minutes and after slows down. In $Fe^{3+}/H_2O_2/UV$ system, the degradation is nearly stopped after about 30 minutes of irradiation. This important slow down and then complete stop of the reaction is due to the almost total consumption of H_2O_2. The higher final removal percentage observed with Fe^{3+} than with Fe(III)-EDDS is due to the presence of EDDS which can consume also HO• and so decrease the reactivity efficiency on *p*-HPA.

As a contrary of this rapid initial degradation observed with H_2O_2, in the Fe(III)-EDDS/$Na_2S_2O_8$/UV system, a gradual degradation during the irradiation process is observed (Fig.1). Fe(III)-EDDS is decomposed fast almost in the first 10 min by photoredox process, into Fe(II) and $EDDS^{\bullet}$, whatever the species present in the solution [14, 30]. In the Fe(III)-EDDS/$Na_2S_2O_8$/UV system $R_{p\text{-HPA}}$ slightly increases until pH 4.0 and then decreases when the pH increases (Fig 4). The pH effect is not exactly the same with H_2O_2 (an increase is observed until around pH 7.5). This difference of pH effect could be due to the interaction of $S_2O_8^{2-}$ in the radical processes. Indeed, $S_2O_8^{2-}$ can react with the first radical generated by the photoredox process on EDDS (R10) and then avoid the reaction with O_2 leading to the formation of $HO_2^{\bullet}/O_2^{\bullet-}$ [44]. This hypothesis was deduced from the literature (Miralles-Cuevas et al. 2014) [12], EDDS• can react with hydroxide anions or persulfate in aqueous solution to form related radicals (i.e. hydroxyl and sulfate radicals). Furthermore, $S_2O_8^{2-}$ can consume electrons and $O_2^{\bullet-}$ to form sulfate radicals [45, 46]. While it's well known that $HO_2^{\bullet}/O_2^{\bullet-}$ are particularly important

because they can modify the Fe(III)/Fe(II) cycle and so the reactivity [34]. Moreover, the degradation efficiency is mainly affected by the photochemical activation abilities of different formed of Fe(III)-EDDS complex and the soluble Fe(III) concentrations in solution [30]. With pH increase, the precipitation of Fe(III) in aqueous solution is became a main limiting step. For another non-negligible reason, it's well known that Fe(II) can be easily oxidized to Fe(III) by the dissolved oxygen in water, and this effect is accelerated when solution pH is higher than 4 [47]. So, the soluble Fe(II) undergoes competitive reaction with H_2O_2/ $S_2O_8^{2-}$ or dissolved oxygen. From R1 and R3, $k_{S_2O_8^{2-},Fe^{2+}}$ is smaller than $k_{H_2O_2,Fe^{2+}}$, and we argue that in the competing reactions, high amount of Fe(II) can be consumed by oxygen in Fe(III)-EDDS/$Na_2S_2O_8$/UV systems at higher pH's solutions. This reactivity can explain the decreased degradation rate when the pH increases. Comparison between Fe^{3+} and Fe(III)-EDDS also was conducted, as shown in Fig.S5. At pH 2.0, Fe^{3+}/$Na_2S_2O_8$ (500 μM)/UV system shows a fast and gradual degradation of *p*-HPA, and *p*-HPA can be removed completely in 45 min.

3.6 Identification of active species at pH 3.9

In order to determine the radicals involved in the degradation of *p*-HPA in the different processes, IPA and TBA are used as scavengers of radicals and so added in the solution (Fig.5). In fact, at adopted concentrations, IPA (10 or 20 mM) was considered to quench efficiently both generated $SO_4^{\bullet-}$ and $HO^{\bullet}$, considering the second order rate constants of $k_{IPA,SO_4^{\bullet-}}$ = 7.42 × 10^7 M^{-1} s^{-1} and $k_{IPA,HO^{\bullet}}$ = 1.9 × 10^9 M^{-1} s^{-1}, while TBA (1 or 2 mM) can be considered to be more selective toward $HO^{\bullet}$ ($k_{TBA,HO^{\bullet}}$ = 6.0 × 10^8 M^{-1} s^{-1}) than with $SO_4^{\bullet-}$ ($k_{TBA,SO_4^{\bullet-}}$ = 8.31 × 10^5 $M^{-}1$ s^{-1}) [39]. From Fig.5A, 20 mM of IPA can almost completely inhibit the degradation of *p*-HPA. At this

concentration, 97 % of $HO^{\bullet}$ is consumed by IPA and only 3% was consumed by *p*-HPA. At lower concentration of IPA (1 mM) only 63% of $HO^{\bullet}$ can react with IPA and so a degradation of *p*-HPA was still observed and corresponds to almost 30% of removal. So, $HO^{\bullet}$ radical is identified as the active species responsible of *p*-HPA transformation in the system with H_2O_2.

In the presence of persulfate (500 µM), 20 mM of IPA can react with 86% $SO_4^{\bullet-}$ when *p*-HPA is present at 50 µM, so higher concentrated IPA is needed if $SO_4^{\bullet-}$ want to be completely inhibited. $HO^{\bullet}$ radical is mainly generated from two routes. Firstly, it is generated from the photolysis of Fe(III)-EDDS complex. Secondly, $SO_4^{\bullet-}$ can also react with hydroxyl anion or water molecule to produce $HO^{\bullet}$ (R13-14) [17, 48, 49]. To evaluate the relative significance of the two radicals (sulfate and hydroxyl) in this system, experiments are also performed with TBA acting specifically as a trap for hydroxyl radical. When the concentration of TBA increases from 1 to 2 mM the decrease of *p*-HPA concentration near 60% is the same (Fig. 5B). So, it is possible to conclude both radicals are involved in the system Fe(III)-EDDS/$Na_2S_2O_8$/UV with a specific percentage respectively near 20% for $HO^{\bullet}$ and 80% for $SO_4^{\bullet-}$.

$SO_4^{\bullet-}+OH^- \rightarrow SO_4^{2-}+HO^{\bullet}$ $\quad k = (6.5\pm1.0)\times10^7\ M^{-1}\ s^{-1}$ (R13)

$SO_4^{\bullet-}+H_2O \rightarrow SO_4^{2-}+HO^{\bullet}+H^+$ $\quad k = 11.92\ M^{-1}\ s^{-1}$ (R14)

4 Conclusion : comparison of H_2O_2 and $S_2O_8^{2-}$ efficiency

In general, the *p*-HPA degradation efficiency is much higher with Fe(III)-EDDS/H_2O_2/UV system than with Fe(III)-EDDS/$Na_2S_2O_8$/UV system whatever the solution pH's. Firstly, this difference can be explained considering the second order rate constants $k_{p-HPA,HO^{\bullet}}$ and $k_{p-HPA,SO_4^{\bullet-}}$ (Table 1). The value of $k_{p-HPA,HO^{\bullet}}$ is higher than $k_{p-HPA,SO_4^{\bullet-}}$ both at pH 2.5 (4.6

times) and 8.5 (2.1 times). Secondly, the rate constants of the key reactions generating the radical species is more than 3 times higher for the Fenton process (R1) than for the activation of persulfate with Fe(II) (R3). However, at pH 2.5, the ratio of the rate constants between radical species and *p*-HPA $k_{p-HPA,HO^{\bullet}} / k_{p-HPA,SO_4^{\bullet-}}$ equal to 4.6 and the ratio of *p*-HPA disappearance rate in the two systems $R_{p\text{-HPA}}$ (H_2O_2)/ $R_{p\text{-HPA}}$ ($Na_2S_2O_8$) equal to 5.2 are similar. It is slightly higher for the *p*-HPA disappearance rate which is coherent with the two reasons mentioned at the beginning of this paragraph. As a contrary the difference between these two ratios is much higher at pH 8.5, $R_{p\text{-HPA}}$ (H_2O_2)/$R_{p\text{-HPA}}$ ($Na_2S_2O_8$) equal to 16.7 is eight times higher than $k_{p-HPA,HO^{\bullet}} / k_{p-HPA,SO_4^{\bullet-}}$ equal to 2.1. So, as previously demonstrated, the Fenton process, involving Fe(III)-EDDS complex, is higher at near neutral pH than in acidic pH [34]. This significant result in terms of environmental aquatic compartments seems not present for the activation of persulfate to generate $SO_4^{\bullet-}$ radical. Indeed, in this case a dramatic decrease of the efficiency is observed. So, in this particular study, with *p*-HPA used as organic pollutant and UV/Fe(III)EDDS as source of Fe(II), we clearly demonstrated that the Fenton process is more efficient than activation of persulfate process and more particularly at environmentally closed pH values.

In the future, the application of such AOP's using Fe(III)EDDS complexes could be also studied in real water matrix such as sewage treatment plant (STP) waters. However, it is very well known that the presence of naturally occurring inorganic ions and organic matter can play very often an inhibition role on the pollutant degradation. In fact, as recently demonstrated in STP waters, the formation of secondary radicals such as carbonate ($CO_3^{\bullet-}$) and chloride derivative ($Cl^{\bullet}$, $Cl_2^{\bullet-}$,…) can strongly modify the oxidative process and as consequence the pollutant degradation [39, 50].

Acknowledgement:

This Special Issue is dedicated to honor the retirement of Prof. César Pulgarin at the Swiss Federal Institute of Technology (EPFL, Switzerland), a key figure in the area of Catalytic Advanced Oxidation Processes. The authors gratefully acknowledge financial support from China Scholarship Council for Xiaoning Wang to study at the University Clermont Auvergne, France. This work was supported by the National Natural Science Foundation of China (NSFC 21077027), Science and Technology Commission of Shanghai Municipality (STCSM 12230706900). Authors acknowledge financial support from the Region Council of Auvergne, from the "Féderation des Recherches en Environnement" through the CPER "Environment" founded by the Region Auvergne, the French government, FEDER from the European Community from PRC program CNRS/NSFC n°270437 and from CAP 20-25 I-site project.

Reference:

[1] R. Andreozzi, V. Caprio, A. Insola, R. Marotta, Catal. Today 53 (1999) 51-59.
[2] J.J. Pignatello, E. Oliveros, A. MacKay, Crit. Rev. Env. Sci. Tec. 36 (2006) 1-84.
[3] D. Huang, C. Hu, G. Zeng, M. Cheng, P. Xu, X. Gong, R. Wang, W. Xue, Sci. Total Environ. 574 (2017) 1599-1610.
[4] M.K. Sherwood, D.P. Cassidy, Chemosphere 113 (2014) 56-61.
[5] W. Huang, M. Brigante, F. Wu, K. Hanna, G. Mailhot, Environ. Sci. Poll. Res. 20 (2013) 39-50.
[6] S. Giannakis, S. Liu, A. Carratalà, S. Rtimi, M. Bensimon, C. Pulgarin, Appl. Catal., B 204 (2017) 156-166.
[7] W. Huang, M. Brigante, F. Wu, K. Hanna, G. Mailhot, J. Photochem. Photobiol., A 239 (2012) 17-23.
[8] L. Santos-Juanes, F.S. García Einschlag, A.M. Amat, A. Arques, Chem. Eng. J. 310 (2017) 484-490.
[9] Y. Wu, M. Passananti, M. Brigante, W. Dong, G. Mailhot, Environ. Sci. Poll. Res. 21 (2014) 12154-12162.
[10] Y. Wu, H. Yuan, G. Wei, S. Zhang, H. Li, W. Dong, Environ. Sci. Poll. Res. 20 (2013) 3-9.
[11] R. Andreozzi, V. Caprio, R. Marotta, D. Vogna, Water Res. 37 (2003) 993-1004.
[12] S. Miralles-Cuevas, F. Audino, I. Oller, R. Sánchez-Moreno, J.A. Sánchez Pérez, S. Malato, Sep. Purif. Technol. 122 (2014) 515-522.
[13] A. Rastogi, S.R. Al-Abed, D.D. Dionysiou, Water Res. 43 (2009) 684-694.

[14] Y. Wu, A. Bianco, M. Brigante, W. Dong, P. de Sainte-Claire, K. Hanna, G. Mailhot, Environ. Sci. Technol. 49 (2015) 14343-14349.
[15] M. Nie, Y. Yang, Z. Zhang, C. Yan, X. Wang, H. Li, W. Dong, Chem. Eng. J. 246 (2014) 373-382.
[16] D. Han, J. Wan, Y. Ma, Y. Wang, Y. Li, D. Li, Z. Guan, Chem. Eng. J. 269 (2015) 425-433.
[17] J. Li, G. Mailhot, F. Wu, N. Deng, J. Photochem. Photobiol., A 212 (2010) 1-7.
[18] M. Nie, C. Yan, M. Li, X. Wang, W. Bi, W. Dong, Chem. Eng. J. 279 (2015) 507-515.
[19] J. De Laat, H. Gallard, Environ. Sci. Technol. 33 (1999) 2726-2732.
[20] C. Walling, A. Goosen, J. Amer. Chem. Soc. 95 (1973) 2987-2991.
[21] R. Woods, I.M. Kolthoff, E.J. Meehan, J. Amer. Chem. Soc. 86 (1964) 1698-1700.
[22] D.Y. Yan, I.M. Lo, Environ. Pollut. 178 (2013) 15-22.
[23] K. Ylivainio, Environ. Pollut. 158 (2010) 3194-3200.
[24] F.G. Kari, S. Hilger, S. Canonica, Environ. Sci. Technol. 29 (1995) 1008-1017.
[25] C. Bretti, R.M. Cigala, C. De Stefano, G. Lando, S. Sammartano, Chemosphere 150 (2016) 341-356.
[26] H. Cui, X. Gu, S. Lu, X. Fu, X. Zhang, G.Y. Fu, Z. Qiu, Q. Sui, Chem. Eng. J. 309 (2017) 80-88.
[27] D. Han, J. Wan, Y. Ma, Y. Wang, M. Huang, Y. Chen, D. Li, Z. Guan, Y. Li, Chem. Eng. J. 256 (2014) 316-323.
[28] S. Papoutsakis, F.F. Brites-Nóbrega, C. Pulgarin, S. Malato, J. Photochem. Photobiol., A 303-304 (2015) 1-7.
[29] S. Papoutsakis, S. Miralles-Cuevas, I. Oller, J.L. Garcia Sanchez, C. Pulgarin, S. Malato, Catal. Today 252 (2015) 61-69.
[30] Y. Wu, M. Brigante, W. Dong, P. de Sainte-Claire, G. Mailhot, J. Phys. Chem. A 118 (2014) 396-403.
[31] X. Zhang, X. Gu, S. Lu, Z. Miao, M. Xu, X. Fu, Z. Qiu, Q. Sui, Chemosphere 160 (2016) 1-6.
[32] P. Soriano-Molina, J.L. García Sánchez, O.M. Alfano, L.O. Conte, S. Malato, J.A. Sánchez Pérez, Appl. Catal., B 233 (2018) 234-242.
[33] S. Satyro, M. Race, F. Di Natale, A. Erto, M. Guida, R. Marotta, Chem. Eng. J. 283 (2016) 1484-1493.
[34] W. Huang, M. Brigante, F. Wu, C. Mousty, K. Hanna, G. Mailhot, Environ. Sci. Technol. 47 (2013) 1952-1959.
[35] M.A. Miranda, M.a.L. Marín, A.M. Amat, A. Arques, S. Seguí, Appl. Catal., B 35 (2002) 167-174.
[36] I. Sanchez, F. Stüber, A. Fabregat, J. Font, A. Fortuny, C. Bengoa, J. Hazard. Mater. 199–200 (2012) 328-335.
[37] D. Dulin, T. Mill, Environ. Sci. Technol. 16 (1982) 815-820.
[38] M. Brigante, T. Charbouillot, D. Vione, G. Mailhot, J. Phys. Chem. A 114 (2010) 2830-2836.
[39] Y. Wu, R. Prulho, M. Brigante, W. Dong, K. Hanna, G. Mailhot, J. Hazard. Mater. 322 (2017) 380-386.
[40] Y. Ji, C. Ferronato, A. Salvador, X. Yang, J.-M. Chovelon, Sci. Total Environ. 472 (2014) 800-808.
[41] Y. Zhang, N. Klamerth, S.A. Messele, P. Chelme-Ayala, M. Gamal El-Din, J. Hazard. Mater. 318 (2016) 371-378.
[42] I. Di Somma, L. Clarizia, S. Satyro, D. Spasiano, R. Marotta, R. Andreozzi, Chem. Eng. J. 270 (2015) 519-527.
[43] T.J. Hardwick, Can. J. Chem. 35 (1957) 428-436.
[44] O. Abida, G. Mailhot, M. Litter, M. Bolte, Photochem. Photobiol. Sci. 5 (2006) 395-402.
[45] G.V. Buxton, C.L. Greenstock, W.P. Helman, A.B. Ross, J. Phys. Chem. Ref. Data 17 (1988) 513-886.
[46] G.-D. Fang, D.D. Dionysiou, S.R. Al-Abed, D.-M. Zhou, Appl. Catal., B 129 (2013) 325-332.

[47] B. Morgan, O. Lahav, Chemosphere 68 (2007) 2080-2084.
[48] G.-D. Fang, D.D. Dionysiou, D.-M. Zhou, Y. Wang, X.-D. Zhu, J.-X. Fan, L. Cang, Y.-J. Wang, Chemosphere 90 (2013) 1573-1580.
[49] P. Neta, R.E. Huie, A.B. Ross, J. Phys. Chem. Ref. Data 17 (1988) 1027-1284.
[50] W. Huang, A. Bianco, M. Brigante, G. Mailhot, J. Hazard. Mater. 347 (2018) 279-287.

Table 1 Second order constant of hydroxyl and sulfate radicals with *p*-HPA under its molecular (pH 2.5) and mono-anionic (pH 8.5) forms.

	pH=2.5 (Molecular form)	pH=8.5 (Mono-anionic form)
$k_{p-HPA,HO^{\bullet}}$ (M^{-1} s^{-1})	$(2.2\pm0.1)\times10^{10}$	$(7.3\pm0.3)\times10^{9}$
$k_{p-HPA,SO_4^{\bullet-}}$ (M^{-1} s^{-1})	$(4.8\pm0.1)\times10^{9}$	$(3.5\pm0.1)\times10^{9}$

Figures Caption

Fig.1 (**A**) Concentration change of *p*-HPA in the Fenton and photo-Fenton systems with different amounts of H_2O_2 added, (**B**) Degradation of *p*-HPA with different $Na_2S_2O_8$ concentrations with and without UV. [*p*-HPA] = 50 μM, [Fe(III)-EDDS] = 100 μM, pH = 3.9.

Fig.2 (**A**) H_2O_2 concentration effect on the initial degradation rate of *p*-HPA in photo-Fenton system at pH = 7.5, (**B**) $Na_2S_2O_8$ concentration effect on the initial degradation rate of *p*-HPA in Fe(III)-EDDS/$Na_2S_2O_8$/UV system at pH = 3.9 . [*p*-HPA] = 50 μM, [Fe(III)-EDDS] = 100 μM, irradiation time considered to evaluate the degradation rate = 5 min.

Fig.3 (**A**) Fe(III)-EDDS concentration effect on the removal percentage of *p*-HPA in photo-Fenton system after 5 min of irradiation. [*p*-HPA] = 50 μM, [H_2O_2] = 100 μM, pH = 7.5. (**B**) Fe(III)-EDDS concentration effect on the removal percentage of *p*-HPA in Fe(III)-EDDS/$Na_2S_2O_8$/UV system after 5 min of irradiation. [*p*-HPA] = 50 μM, [$Na_2S_2O_8$] = 500 μM, pH = 3.9.

Fig.4 pH effect on the initial degradation rate of *p*-HPA in Fe(III)-EDDS/H_2O_2/UV and Fe(III)-EDDS/$Na_2S_2O_8$/UV systems. [*p*-HPA] = 50 μM, [Fe(III)-EDDS] = 100 μM , [H_2O_2] = 100 μM, [$Na_2S_2O_8$] = 100 μM, irradiation time considered to evaluate the degradation rate = 5min. Insert: Removal percentage of *p*-HPA in Fe(III)-EDDS/UV system after 120 min of irradiation at different pH. [Fe(III)-EDDS] = 100 μM, [p-HPA] = 50 μM.

Fig.5 (**A**) Kinetic of *p*-HPA concentration when different concentrations of isopropanol were added to the photo-Fenton process. [*p*-HPA] = 50 μM, [H_2O_2] = 100 μM, [Fe(III)-EDDS] = 100 μM, pH = 3.9 under UV. (**B**) Kinetic of *p*-HPA concentration when different concentrations of isopropanol or tert-butyl alcohol were added to the Fe(III)-EDDS/$Na_2S_2O_8$/UV process. [*p*-HPA] = 50 μM, [$Na_2S_2O_8$] = 500 μM, [Fe(III)-EDDS] = 100 μM, pH = 3.9.

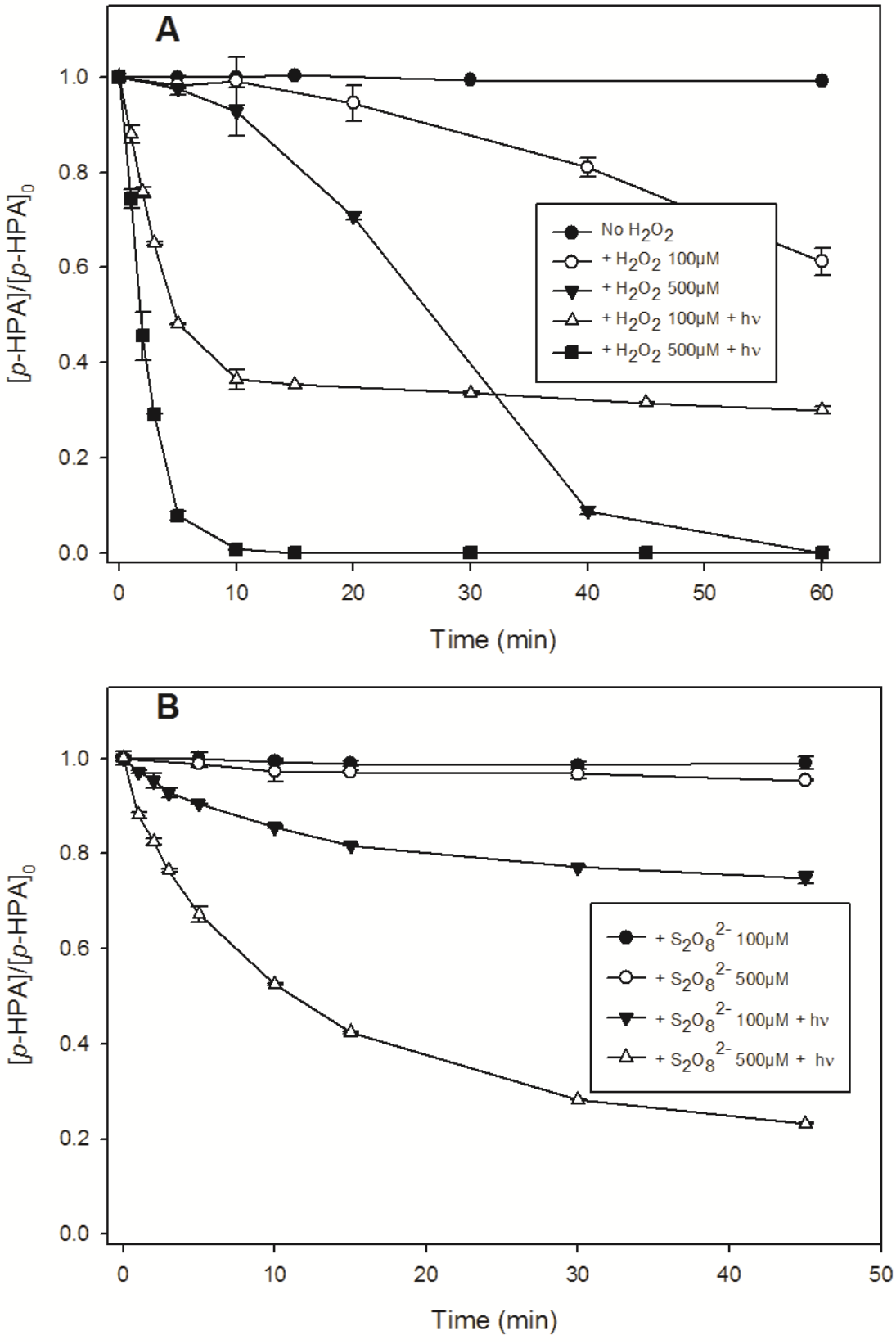
A
1.0
0.8
0.6
0.4
0.2
0.0
[p-HPA]/[p-HPA]0
0
10
20
30
40
50
60
Time (min)
No H2O2
+ H2O2 100μM
+ H2O2 500μM
+ H2O2 100μM + hν
+ H2O2 500μM + hν
B
1.0
0.8
0.6
0.4
0.2
0.0
[p-HPA]/[p-HPA]0
0
10
20
30
40
50
Time (min)
+ S2O8 2- 100μM
+ S2O8 2- 500μM
+ S2O8 2- 100μM + hν
+ S2O8 2- 500μM + hν

Fig.1

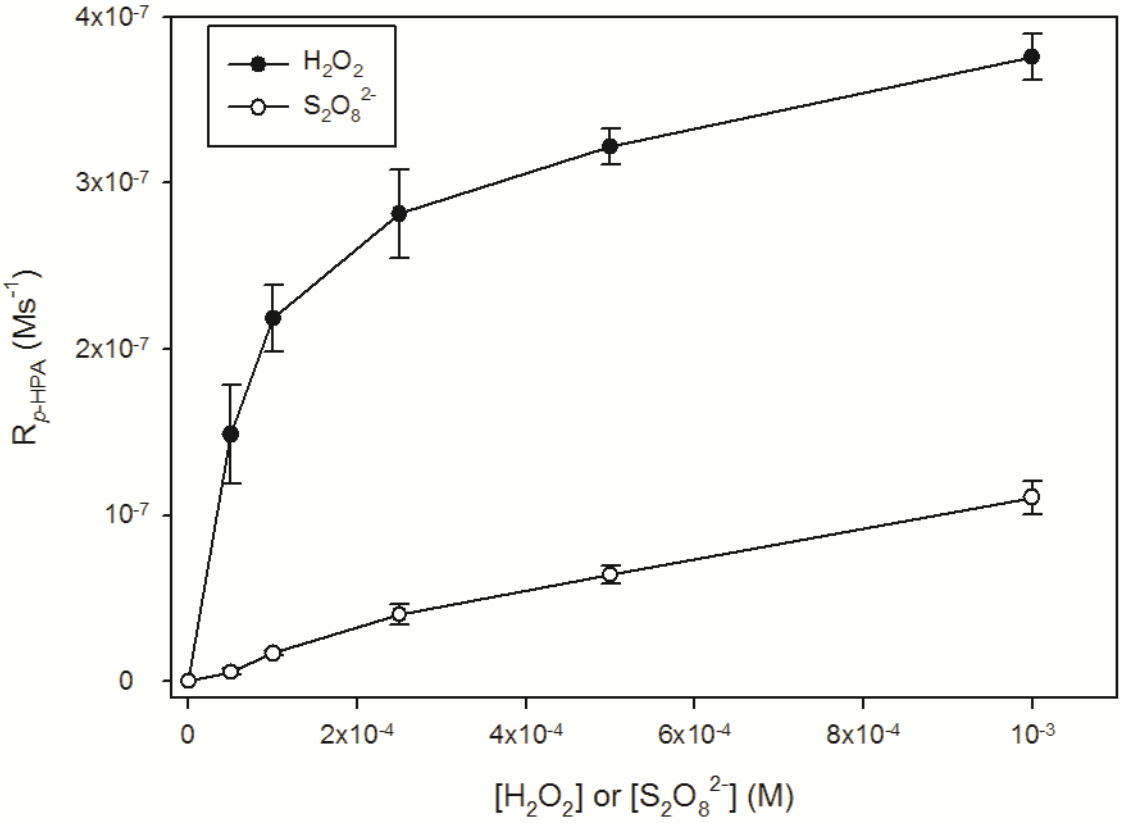
4x10-7
3x10-7
2x10-7
10-7
0
R p-HPA (Ms-1)
H2O2
S2O8 2-
0
2x10-4
4x10-4
6x10-4
8x10-4
10-3
[H2O2] or [S2O8 2-] (M)

Fig.2

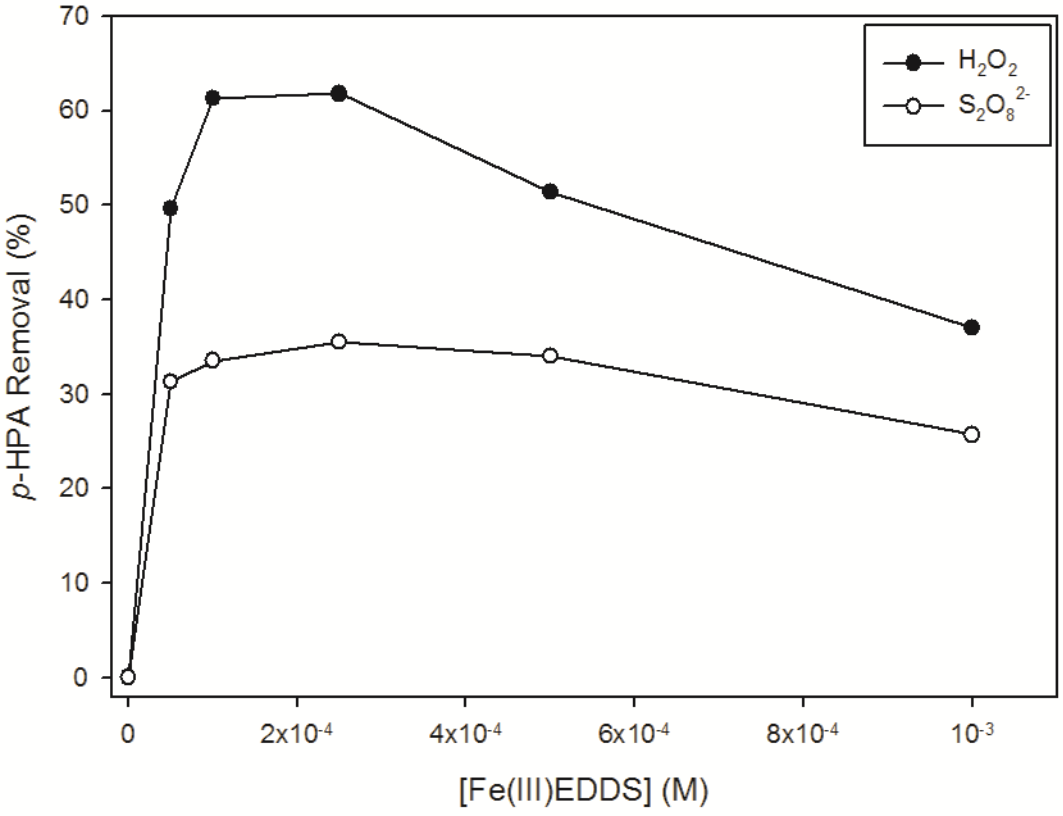
70
60
50
40
30
20
10
0
p-HPA Removal (%)
0
2x10-4
4x10-4
6x10-4
8x10-4
10-3
[Fe(III)EDDS] (M)
H2O2
S2O8 2-

Fig.3

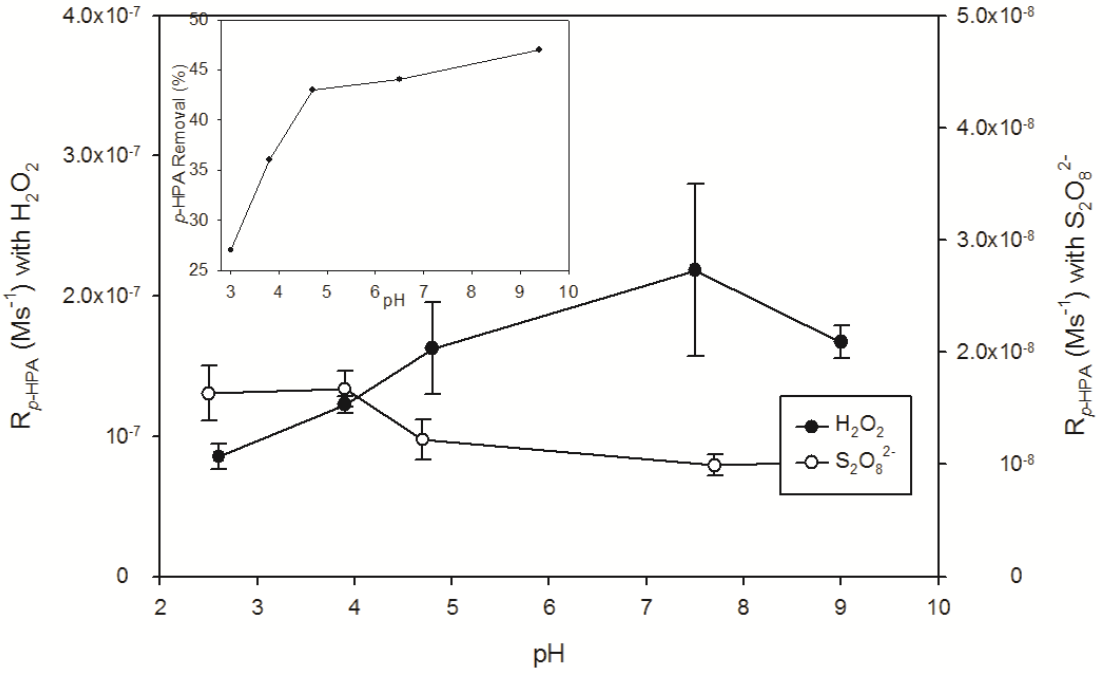
4.0x10-7
3.0x10-7
2.0x10-7
10-7
0
RP-HPA (Ms-1) with H2O2
5.0x10-8
4.0x10-8
3.0x10-8
2.0x10-8
10-8
0
RP-HPA (Ms-1) with S2O8 2-
2
3
4
5
6
7
8
9
10
pH
H2O2
S2O8 2-
p-HPA Removal (%)
50
45
40
35
30
25
pH

Fig.4.

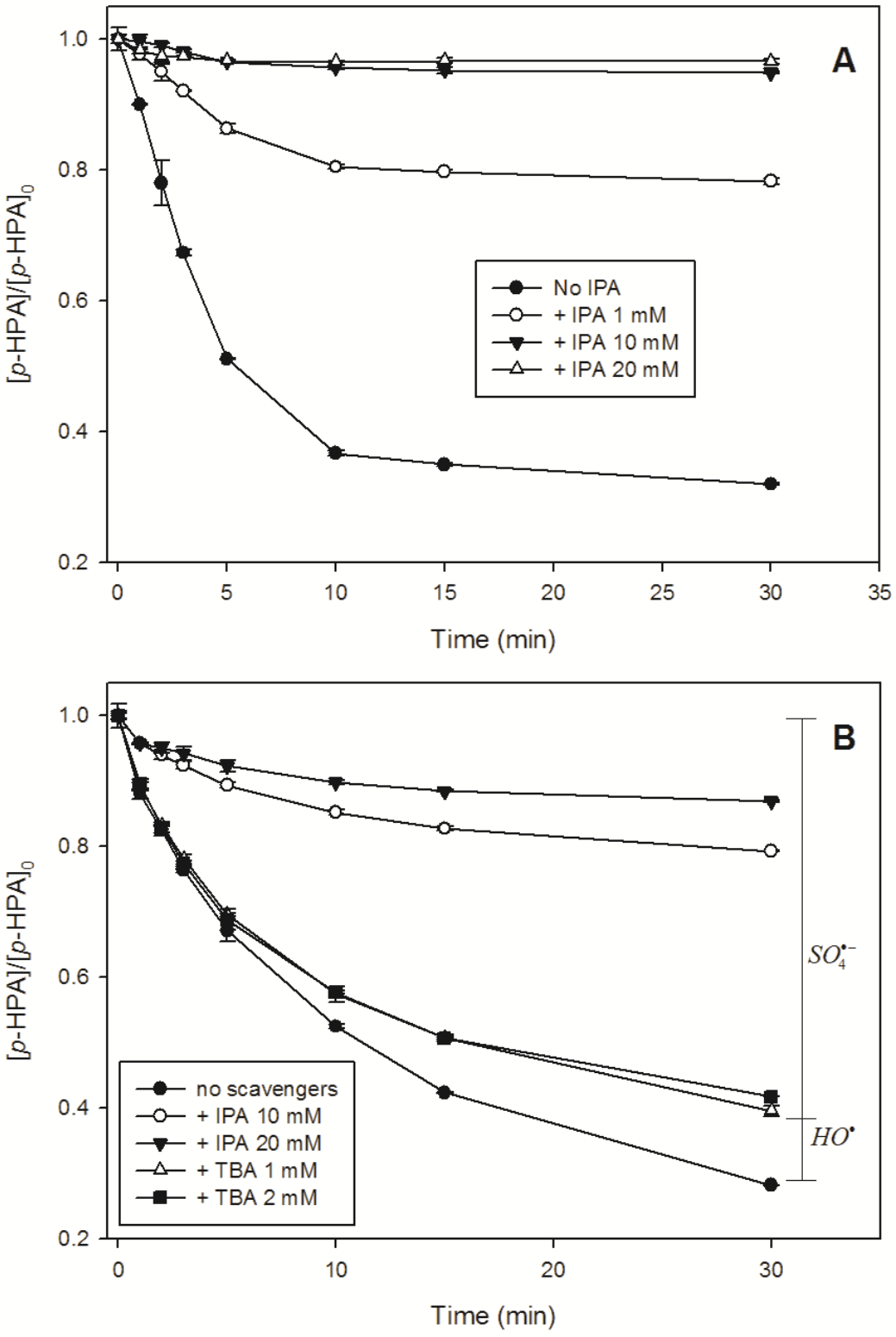
A
[p-HPA]/[p-HPA]0
Time (min)
No IPA
+ IPA 1 mM
+ IPA 10 mM
+ IPA 20 mM
B
[p-HPA]/[p-HPA]0
Time (min)
no scavengers
+ IPA 10 mM
+ IPA 20 mM
+ TBA 1 mM
+ TBA 2 mM
$SO_4^{\bullet-}$
$HO^{\bullet}$

Fig.5